

# Experimental Results for Electron Bernstein Wave Heating in the Large Helical Device<sup>\*)</sup>

Hiroe IGAMI, Shin KUBO, Takashi SHIMOZUMA, Yasuo YOSHIMURA, Hiromi TAKAHASHI, Hiroshi IDEI<sup>1)</sup>, Masaki NISHIURA, Shinya OGASAWARA<sup>2)</sup>, Ryohei MAKINO<sup>2)</sup>, Ryuhei KUMAZAWA, Takashi MUTOH, Akio SAGARA and Takuya GOTO

*National Institute for Fusion Science, Toki 509-5292, Japan*

<sup>1)</sup>*Research Institute for Applied Mechanics, Kyushu University, Kasuga 816-8580, Japan*

<sup>2)</sup>*Department of Energy and Technology, Nagoya University, Nagoya 464-8463, Japan*

(Received 12 December 2011 / Accepted 16 April 2012)

Electron cyclotron heating (ECH) using electron Bernstein waves (EBWs) was studied in the large helical device (LHD). Oblique launching of the slow extraordinary (SX-) mode from the high field side and oblique launching of the ordinary (O-) mode from the low field side were adopted to excite EBWs in the LHD by using electron cyclotron (EC) wave antennas installed apart from the plasma surface. Increases in the stored energy and electron temperature were observed for both cases of launching. These launching methods for ECH using EBWs (EBWH) is promising for high-density operation in future helical fusion devices instead of conventional ECH by normal electromagnetic modes.

© 2012 The Japan Society of Plasma Science and Nuclear Fusion Research

Keywords: electron cyclotron heating, electron Bernstein wave, mode conversion process, high-density operation, heating in fusion device

DOI: 10.1585/pfr.7.2402110

## 1. Introduction

As a heating method in fusion devices, electron cyclotron heating (ECH) has a great advantage; that is, the electron cyclotron (EC) wave antennas can be installed apart from the plasma surface. However, for high-density operation in a helical fusion reactor [1], normal electromagnetic modes cannot access the electron cyclotron resonance (ECR) layer, because the electron density is larger than the cutoff density. Conversely, electron Bernstein waves (EBWs) have no density limit in propagation and are absorbed in the ECR layer by cyclotron damping. Thus, at high-density operation, electron Bernstein wave heating (EBWH) is expected to replace conventional ECH by normal electromagnetic modes. EBWs are excited in the upper hybrid resonance (UHR) layer via the mode conversion process from the slow extraordinary (SX-) mode. Therefore, the electromagnetic waves must be launched from outside the plasma to couple it with the SX-mode inside the plasma.

Experimentally studying EBWH with antennas installed apart from the plasma surface is important for understanding its application in future fusion devices. In the large helical device (LHD), two methods of EBWH with quasi-optical mirror antennas installed apart from the plasma surface have been experimentally studied [2–4]. One method is to launch the SX-mode obliquely to the ex-

ternal magnetic field from the high field side with the lower port antenna [2, 4]. The other method is to launch the ordinary (O-) mode obliquely to the external magnetic field from the low field side [3, 5].

This study reports progress on the experimental study of these two methods in the LHD. Section 2 presents experimental results for the oblique launching of the SX-mode in a relatively high-density that is still less than the cutoff density. Section 3 presents experimental results for the oblique launching of the O-mode. In Section 4, we summarize our results and briefly discuss applications to a helical fusion device.

## 2. Oblique Launching of the SX-Mode

Figure 1 shows a schematic of the oblique launching of the SX-mode from the lower port antenna in the LHD. The electromagnetic waves are launched obliquely upward with a large toroidal angle with the polarization of the extraordinary (X-) mode; therefore, at first the launched X-mode propagates obliquely to the external magnetic field. The launched X-mode passes near the vacuum vessel wall in the near side of the center of the torus and first encounters the right-handed cutoff (RC) in front of the exterior ECR layer outside the last closed flux surface (LCFS) from the low field side. The electron density and temperature are very low there and the width of the evanescent region between the RC and the UHR layer is very thin; therefore, the launched X-mode may transmit through the region by the

author's e-mail: igami@lhd.nifs.ac.jp

<sup>\*)</sup> This article is based on the presentation at the 21st International Toki Conference (ITC21).

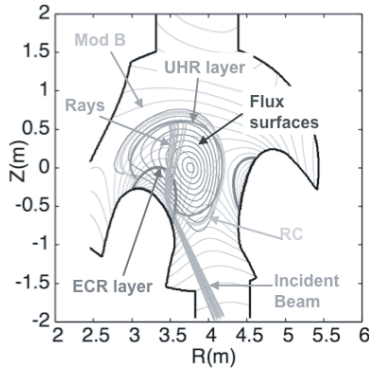


Fig. 1 Contours of mod B, flux surfaces, the UHR layer, the ECR layer, and the RC plotted on the plane that is parallel to the z-axis and includes the antenna position and launching vector. Projections of the rays on this plane are also plotted.

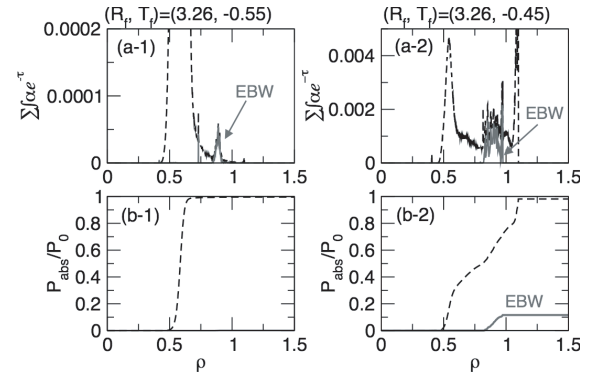


Fig. 3 Profiles of the local absorbed power (a-1 and a-2) and integrated absorbed power normalized by the launched power (b-1 and b-2) for different launching directions ( $R_f$ ,  $T_f$ ). The solid line indicates the absorption of EBWs, and the dashed line indicates the total absorption of EBWs and the SX-mode.

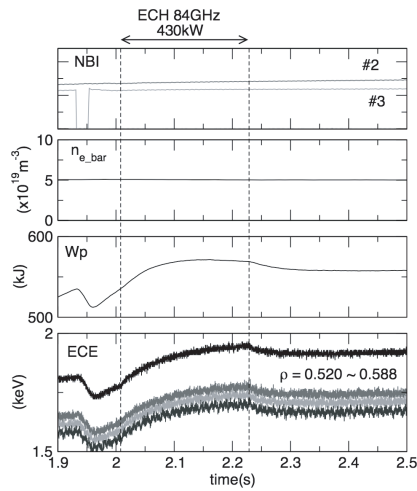


Fig. 2 Time dependences of the following variables (from the top): NBI pulses, line-averaged density, stored energy, and ECE signals.

tunneling effect and reaches the exterior ECR layer. Power absorption in the exterior ECR layer is expected to be very weak; therefore, the X-mode reaches the high field side of the exterior ECR layer, enters the LCFS, and then approaches the interior ECR layer as the SX-mode. If the SX-mode is not completely absorbed in the interior ECR layer, it can reach the UHR layer and is mode converted to EBWs.

Figure 2 shows discharge waveforms when an 84 GHz, 0.43 MW millimeter wave was launched obliquely with the polarization of the X-mode. The magnetic configuration was  $(R_{ax}, B_t) = (3.7 \text{ m}, 2.675 \text{ T})$ , where  $R_{ax}$  is the position of the magnetic axis, and  $B_t$  is the magnetic field strength at the magnetic axis. The target hydrogen plasma was sustained by neutral beam injection (NBI). The stored energy and electron temperature measured by electron cyclotron emission (ECE) radiometer increased after turning on the ECH power. The heating

efficiency estimated from the difference of the temporal differentiation of the stored energy before and after turning off the ECH power was 22.5%. The electron density was less than the cutoff density ( $8.74 \times 10^{19} \text{ m}^{-3}$ ); therefore, there were two possible mechanisms for ECH: (1) fundamental SX-mode heating and (2) EBWH. A previous numerical study with ray-tracing calculation suggested that as the electron density at the fundamental ECR layer increases, power absorption of the SX-mode decreases, and the launched SX-mode can cross the fundamental ECR layer without complete power absorption and reach the UHR layer [4, 6]. In that case, EBWs can be excited and EBWH occurs.

Propagation and power absorption of the wave launched as the SX-mode at first were analyzed by using a multi ray-tracing calculation, in which the density profile  $n_e(\rho) = 4.7 \cdot (1.0 - (\rho/1.1)^8)^2 (\times 10^{19} \text{ m}^{-3})$  and the polynomial-fitted experimental electron temperature profile  $T_e(\rho)$  were used, where  $\rho$  is the normalized minor radius. The calculation started at the high field side of the ECR layer with  $\omega_{ce}/\omega = 1.01$ , where  $\omega_{ce}$  is the electron cyclotron angular frequency, and  $\omega$  is the wave angular frequency. Using the experimental setting of the aiming point of the launched EC wave results in a parallel refractive index  $N_{||}$  of  $\sim 0.55$  at the starting point; however, it varies with propagation because of the inhomogeneity of the external magnetic field. Most of the launched power is absorbed as the SX-mode at the fundamental ECR layer around  $\rho = 0.58$ , where  $N_{||}$  is  $\sim 0.21$ . Very less amount of the SX-mode can reach the UHR layer and is mode converted to EBWs. The EBWs are absorbed around  $\rho = 0.93$  as shown in Figs. 3 (a-1) and (b-1). If the aiming point on the equatorial plane is moved along the toroidal direction toward the antenna by 10 cm,  $N_{||}$  is  $\sim 0.48$  at first and approaches zero at the fundamental ECR layer. In that case, power absorption of the SX-mode weakens, because  $N_{||}$  is

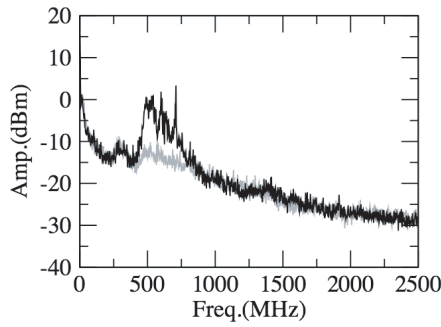


Fig. 4 Frequency spectrum during EC wave launching (black) and the background level (grey) for the same discharge shown in Fig. 2.

close to zero at the ECR layer, and  $\sim 10\%$  of the launched power is mode converted to EBWs and the EBWs are absorbed around  $\rho = 0.8$ , as shown in Figs. 3 (a-2) and (b-2).

If the SX-mode reaches the UHR layer, the nonlinear three-wave coupling process can occur. The parametric decay wave in the lower hybrid (LH) wave frequency range excited in this coupling process was determined by using a discone antenna that measures electric field fluctuations. Figure 4 shows the frequency spectrum of an LH wave along with its harmonics range. As shown in Fig. 1, the rays encounter the UHR layer before and after they enter the LCFS. Misalignment of the toroidal launching angle might increase the power to be mode converted to EBWs in the UHR layer inside the LCFS.

There are possible reasons for the low estimate of the heating efficiency. For example, it is possible that part of the launched beam is lost because it hits the wall. Only power absorption inside the LCFS can increase the stored energy because the energy confinement outside the LCFS is poor. In the case shown in Figs. 3 (a-2) and (b-2), 25% of the launched power is absorbed outside the LCFS. In addition, as suggested in a previous study [4], reflection or mode conversion to EBWs can occur when the launched X-mode first approaches the exterior ECR layer from the low field side. Such phenomena can reduce the incident power.

### 3. Oblique Launching of the O-Mode

The density gradient normalized by the vacuum wavelength of the EC wave is very large in the LHD. Therefore, to excite EBWs by EC wave launching from the low field side, the O-mode must be launched obliquely to the magnetic field with an angle such that the plasma cutoff and the left-handed cutoff are very close. In that case, the O-mode is mode converted to the SX-mode, propagates to the UHR layer, and is mode converted to EBWs (the O-X-B mode conversion process). It has been difficult to determine the effect of heating on the change in the stored energy and electron temperature profile with low-power ECH ( $\sim 300$  kW) in high-density plasmas [3]. We expected to be

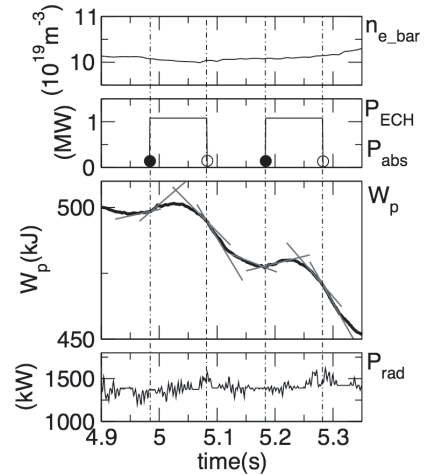


Fig. 5 Time dependences of the following variables (from the top): line-averaged density  $n_{e,\text{bar}}$ ; ECH pulse  $P_{\text{ECH}}$  (solid line) and estimated absorbed power  $P_{\text{abs}}$  (black and white circles); stored energy  $W_p$  (black line) and linear fittings of the stored energy before and after turning on and off of the ECH pulse (grey lines); and radiation loss  $P_{\text{rad}}$ .

able to determine this effect more clearly because of the installation of the high-power ( $\sim 1$  MW) 77 GHz gyrotron.

In previous numerical studies [7, 8] of EBWH via the O-X-B mode conversion process using the existing horizontal port antenna, it was suggested that the power absorption region shifts toward the plasma core as the external magnetic field decreases. However, it was also suggested that the “O-X-B mode conversion window” of the aiming point of the launched EC wave is blocked by the wall of the horizontal port when the magnetic field strength decreases [8]. In our experiment, we first selected the magnetic configuration  $(R_{\text{ax}}, B_t) = (3.75 \text{ m}, 2.2 \text{ T})$  and launched the O-mode. Figure 5 shows the discharge waveforms for our experiment. The target helium plasma was sustained by NBI. The line-averaged density was larger than the cutoff density of 77 GHz ( $7.35 \times 10^{19} \text{ m}^{-3}$ ). As shown in Fig. 5, the gradient of the linear fittings of the stored energy (grey lines) increases after turning on the ECH power and decreases after turning it off. This suggests that the input power to the plasma depends on the ECH power. Radiation loss increases slightly upon turning on the ECH power; however, the effect on the change in the stored energy is insignificant. The heating efficiency estimated from the difference of the temporal differentiation of the stored energy before and after turning on and off the ECH power is  $\sim 15\%$  on an average.

Figure 6 shows a contour plot of the O-X-B mode conversion rate as a function of the aiming point on the virtual upright plane placed at  $R = 3.9$  m (the center of the vacuum vessel); this plot determines the launching direction as  $(T_f, Z_f) = (0.75 \text{ m}, -0.34 \text{ m})$ , which corresponds to the case shown in Fig. 5. Note that  $T_f$  is the distance along the toroidal direction from the horizontally long cross sec-

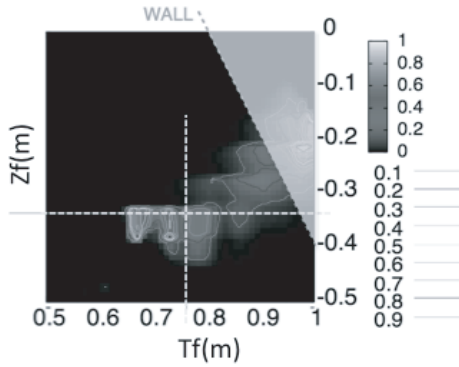


Fig. 6 O-X-B mode conversion rate plotted as a function of the aiming point on the virtual upright plane at  $R = 3.9$  m. The point where the two dashed lines intersect corresponds to the discharge setting shown in Fig. 5.

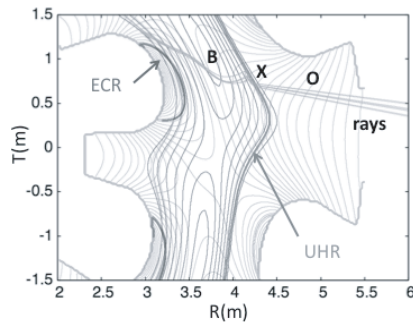


Fig. 7 Projection of the rays onto the plane sliced at  $z = -0.2$  m.

tion, and  $Z_f$  is the distance from the equatorial plane. The O-X-B mode conversion rate  $T_{\text{OXB}}$  was calculated with Eq. (1) [9] (below) at the point where the perpendicular component of the refractive index is at a minimum near the plasma cutoff or the left-handed cutoff in the ray-tracing calculation.

$$T_{\text{OXB}} = \exp \left\{ -\pi(\omega/c)L_n(\beta/2)^{1/2} \times [2(1 + \beta)(N_{\parallel} - N_{\parallel\text{opt}})^2 + N_{\perp}^2] \right\}, \quad (1)$$

$L_n$ : scale length of the density gradient,

$N_{\parallel}$ : parallel refractive index,

$N_{\perp}$ : refractive index perpendicular to the magnetic field and density gradient,

$N_{\parallel\text{opt}} = \{\beta/(1 + \beta)\}^{1/2}$ , where  $\beta = \Omega_{\text{ce}}/\omega$ ,

$\Omega_{\text{ce}}$ : electron cyclotron angular frequency,

$\omega$ : angular frequency.

In the ray-tracing calculation, an electron density profile of  $n_e(\rho) = 8.7 \cdot (1.0 - (\rho/1.0)^{20})^2 \times 10^{19} \text{ m}^{-3}$  was considered. According to Fig. 6,  $T_{\text{OXB}} \sim 20\%$ , which is similar to the estimated heating efficiency obtained with the experimental setting. Figure 7 shows the ray propagation before and after the O-X-B mode conversion. After the mode conversion in the peripheral region, the wave propagates toward the core region. As shown in Fig. 8, a part

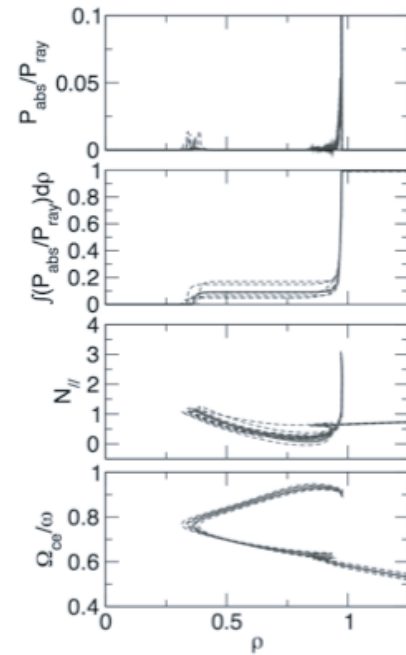


Fig. 8 Radial dependence of the following variables (from the top): local absorbed power, integrated absorbed power normalized by the launched power, parallel component of the refractive index, and electron cyclotron angular frequency normalized by wave angular frequency. Examples of the ray at the beam center and rays at the  $1/e$  radius are plotted.

of the power is absorbed around  $\rho = 0.3$ , and the rest is absorbed around  $\rho = 0.9$  where the Doppler-shifted resonance condition is fulfilled. In a different discharge with  $(T_f, Z_f) = (0.85, -0.37)$ , the electron temperature measured by ECE radiometer in the core region ( $\rho \sim 0.2$ ) increases after the ECH power is turned on. In these experiments, measurement of the parametric decay wave in the LH wave frequency range was not performed. However, the only possible heating mechanism is the EBWH in the Doppler-shifted ECR layer.

## 4. Discussion and Summary

We observed that oblique SX-mode and oblique O-mode launchings increases the stored energy and electron temperature. For oblique SX-mode launching, the spectrum of a parametric decay wave was observed. This suggests that the SX-mode reached the UHR layer and that the condition of EBW excitation was fulfilled, even though the electron density was less than the cutoff density. To check the validity of the procedure used in the ray-tracing calculation, it is important to compare the power absorption region suggested by the numerical calculation with that observed in the experiment. However, in both experiments for SX- and O-mode launchings, the power absorption region has not yet been ascertained. Moreover, the electron temperature and the electron density profiles used in the calculation do not correspond to the experimental profiles

in the peripheral region. Therefore, in the future we will incorporate the three-dimensional profiles that correspond to the equilibrium data based on the real experimental discharge.

For oblique launching of the SX-mode in future fusion devices, to ensure that the launched beam does not hit the wall, a certain amount of clearance between the plasma edge and vacuum vessel wall is required (as shown in Fig. 1). In addition, to determine whether oblique launching of the SX-mode is available, the reflection and transmission rates at the evanescent layer should be evaluated quantitatively. For oblique launching of the O-mode, it is important to place the antenna to aim for the mode conversion window. In addition, to efficiently heat the core region, it is important to choose the wave frequency such that the UHR layer is near the core region.

## Acknowledgement

The authors thank the technical staff responsible for ECH at the LHD for their help. This research was mainly supported by budget codes NIFS11ULRR701 and 801, and it was partially supported by a Grant-in-aid for Scientific Research from MEXT JAPAN, 2011 23561006.

- [1] A. Sagara *et al.*, Fusion Eng. Des. **81**, 2703 (2006).
- [2] H. Igami *et al.*, Plasma Fusion Res. **1**, 052 (2006).
- [3] H. Igami *et al.*, Rev. Sci. Instrum. **77**, 10E931 (2006).
- [4] H. Igami *et al.*, Nucl. Fusion **49**, 115005 (2009).
- [5] H.P. Laqua *et al.*, Phys. Rev. Lett. **78**, 3467 (1997).
- [6] H. Igami *et al.*, Plasma Sci. Technol. **11-4**, 430 (2009).
- [7] K. Nagasaki and N. Yanagi, Plasma Phys. Control. Fusion **44**, 409 (2002).
- [8] H. Igami *et al.*, Fusion Sci. Technol. **58-1**, 551 (1997).
- [9] E. Mjølhus, J. Plasma Phys. **31**, 7 (1984).